

EMSL Report
November/December 2003

The W.R. Wiley Environmental Molecular Sciences Laboratory (EMSL) is a U.S. Department of Energy (DOE) national scientific user facility located at Pacific Northwest National Laboratory (PNNL) in Richland, Washington. EMSL is operated by PNNL for the DOE Office of Biological and Environmental Research. At one location, EMSL offers a comprehensive array of leading-edge resources in six research facilities.

Access to the capabilities and instrumentation in EMSL facilities is obtained on a peer-reviewed proposal basis. Users are participants on accepted proposals. Staff members work with users to expedite access to the facilities and scientific expertise. The Monthly Report documents research and activities of EMSL staff and users.

Research Highlights

Probing the Intrinsic Electronic Structure of the Cubane [4Fe-4S] Cluster: Nature's Favorite Cluster for Electron Transfer

X Wang,^(a,b) S Niu,^(c,d) X Yang,^(b) SK Ibrahim,^(e) CJ Pickett,^(e) T Ichiye,^(c,d) and LS Wang^(a,b)

(a) Pacific Northwest National Laboratory, Richland, Washington

(b) Washington State University-Tri-Cities, Richland, Washington

(c) Washington State University, Pullman, Washington

(d) Georgetown University, Washington, D.C.

(e) John Innes Centre, Norwich, United Kingdom

Cluster science is a relatively nascent research field that promises a molecular-level understanding of catalysis and discovery of new nanomaterials. However, nature has been using clusters from the beginning of life. Among the important clusters in biochemistry are the iron-sulfur clusters, which constitute the active sites of a growing list of proteins in such essential life-sustaining processes as respiration, nitrogen fixation, and photosynthesis.

The most prototypical and ubiquitous iron-sulfur cluster is the cubane-type [4Fe-4S] cluster, which, in addition to its catalytic and regulatory roles, appears to be nature's most favorite agent for electron transfer and storage, such as in ferredoxins, high-potential proteins, and the integral machineries of hydrogenases and nitrogenases. In proteins, the cubane [4Fe-4S] unit is usually coordinated by the amino acid cysteine (Figure 1). The [4Fe-4S] core functions as an electron transfer agent usually between the following oxidation states: $[4\text{Fe-4S}]^{1+} \leftrightarrow [4\text{Fe-4S}]^{2+} \leftrightarrow [4\text{Fe-4S}]^{3+}$. A fourth state, the all-ferrous species $[4\text{Fe-4S}]^0$, has also been detected in the iron protein of nitrogenase. It is important to understand the intrinsic electronic structure of the iron-sulfur

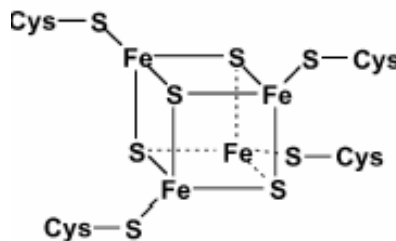


Figure 1. Schematic structure of the [4Fe-4S] active site in proteins.

clusters and modifications by their surroundings in order to understand the properties and functionalities of the iron-sulfur proteins.

In this work, electrospray was used to produce a series of gaseous doubly charged cubane-type complexes, $[\text{Fe}_4\text{S}_4\text{L}_4]^{2-}$ ($\text{L} = -\text{SC}_2\text{H}_5, -\text{SH}, -\text{Cl}, -\text{Br}, -\text{I}$) and the selenium-analogues $[\text{Fe}_4\text{Se}_4\text{L}_4]^{2-}$ ($\text{L} = -\text{SC}_2\text{H}_5, -\text{Cl}$), and their electronic structures were probed with photoelectron spectroscopy and density functional calculations. The photoelectron spectral features are similar among all seven species investigated, revealing a weak threshold feature due to the minority spins on the iron centers and confirming the low-spin two-layer model for the $[\text{4Fe-4S}]^{2+}$ core and its “inverted level scheme.” The measured adiabatic detachment energies, which are sensitive to the terminal ligand substitution, provide the intrinsic oxidation potentials of the $[\text{Fe}_4\text{S}_4\text{L}_4]^{2-}$ complexes. The calculations revealed a simple correlation between the electron donor property of the terminal thiolate as well as the bridging sulfide with the variation of the intrinsic redox potentials. These data provide intrinsic electronic structure information of the $[\text{4Fe-4S}]$ cluster and the molecular basis for understanding the protein and solvent effects on the redox properties of the $[\text{4Fe-4S}]$ active sites. Details on this research are published in Wang et al. (2003).

Citation

Wang X, S Niu, X Yang, SK Ibrahim, CJ Pickett, T Ichiye, and LS Wang. 2003 “Probing the Intrinsic Electronic Structure of the Cubane $[\text{4Fe-4S}]$ Cluster: Nature's Favorite Cluster for Electron Transfer and Storage.” *Journal of the American Chemical Society* 125(46):14072-14081.

Chemical Signatures in Thermal Springs: Lessons from Yellowstone and Kamchatka

NW Hinman,^(a) C Wilson,^(a) T Kendall,^(b) T Moore,^(c) and SD Burton^(d)

(a) University of Montana, Missoula, Montana

(b) Harvard University, Cambridge, Massachusetts

(c) University of Delaware, Newark, Delaware

(d) W.R. Wiley Environmental Molecular Sciences Laboratory, Richland, Washington

Many factors drive chemical change in geothermal systems, and the deposits in these systems provide a signature of system conditions. Long-term effects include climatic change, change in location (i.e., continental drift), and volcanic processes (e.g., climatic processes affect the amount of water circulating through the system and, therefore, the amount of heat released as steam and liquid water). Mid-term effects include seasonal processes and human impacts (e.g., interaction between shallow groundwater and deeper thermal water can affect the amount and chemistry of the water reaching the surface). Short-term effects include photochemical and photosynthetic processes (e.g., reduced forms of iron are detected at mid-day because of photochemical processes, and the by-products of such reactions subsequently reduce sulfide concentrations). In general, changes in the pH and redox conditions from alterations in solution composition can impart chemical signatures in deposits formed in geothermal springs (hot springs).

Since chemical changes can affect pH and redox conditions and the element speciation of geothermal springs, it makes sense to pursue signatures of elements affected by these factors. Although many minor elements are affected by changes in conditions, this study focuses on alterations in major element chemistry, in particular the concentration and form of iron, aluminum, and silicon in geothermal springs. The chemistry of one geothermal spring, the Iron Pool at Roadside Springs, has changed since study of the hot spring began in 1996. It provided an excellent opportunity to observe real-time alterations in the same hot spring. The chemistry of other hot springs, Pork Chop Geyser (Norris Geyser Basin, Yellowstone National Park) and Trinoi Geyser (Kamchatka), are used to represent different geothermal spring chemistry that might result over a longer time period.

EMSL nuclear magnetic resonance (NMR) spectrometers were used to run solid-state NMR experiments to observe the atomic environment of two inorganic elements, ^{27}Al and ^{29}Si , present in hot spring material. The ^{27}Al NMR spectra of samples taken from Pork Chop and Trinoi geysers display spectral features that show different quantities of tetrahedrally and octahedrally coordinated aluminum. The spectral differences in silicon environment between Trinoi and Pork Chop geysers are not as pronounced. Solid-state ^{29}Si NMR spectra show two distinct silicon environments: silicon bridging two silicon atoms via oxygen, and silicon bridging three silicon atoms via oxygen. Sinters from both Yellowstone and Kamchatka are a mix of these two silicon structures.

Movement and Dissolution of a Multicomponent, Viscous, Nonaqueous-Phase Liquid in a Fluctuating Water Table System

M Oostrom,^(a) C Hofstee,^(b) and TW Wietsma^(c)

(a) Pacific Northwest National Laboratory, Richland, Washington

(b) Netherlands Institute of Applied Geosciences, TNO-NITG, Utrecht, The Netherlands

(c) W.R. Wiley Environmental Molecular Sciences Laboratory, Richland, Washington

Nonaqueous phase liquids (NAPLs), such as chlorinated solvents and hydrocarbon fuels, are found in the subsurface at many sites. The solubility of NAPLs is usually relatively low and the dissolution is often a kinetic process. As a result, these liquids might form a source of widespread and long-term contamination of groundwater; thus, the presence of NAPLs poses a major environmental problem. Recharge water may come into contact with the liquids and may transport dissolved components downward to aquifers. In addition, dense vapors originating from volatile organic compounds may sink and spread rapidly in the vadose zone. Subsequent partitioning into the groundwater may create extended contaminant plumes.

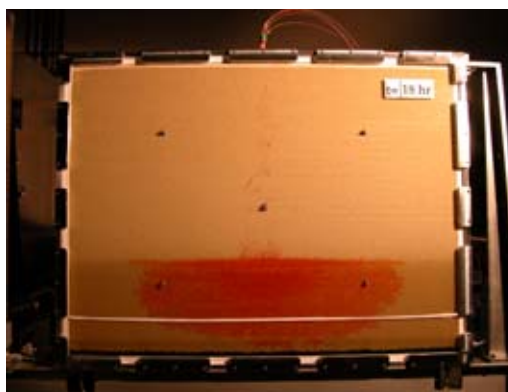


Figure 2. Photograph of a flow cell packed with sand. A NAPL consisting of DBBP, TBP, and lard oil components was introduced and can be seen (in red) as a plume in the water table (dark brown area at bottom third of cell).

Residual NAPL is likely to be present at several contaminated sites. One of the most ubiquitous NAPLs at DOE sites is carbon tetrachloride. At the Hanford Site, an estimated 580 m³ of a multicomponent NAPL containing carbon tetrachloride was disposed to several waste sites. The carbon tetrachloride was disposed with the co-contaminants lard oil, di-butyl-butyl phosphonate (DBBP), and tributyl phosphate (TBP). At present, approximately 65% of the original disposed volume has not been accounted for. A better understanding of science issues related to NAPL movement and dissolution is required to aid in remediation of the Hanford Site.

Typical text book examples of NAPL sources depict a continuous oil body, submersed in the capillary fringe and below the water table. In case of past fluctuations of the groundwater table, the oil lens is assumed to overlie a so-called smearing zone, characterized by water-entrapped discontinuous lenses. This ideal behavior may be compromised when the NAPL has a viscosity larger than water. In addition, most experiment studies on multifluid flow have been limited to single component NAPLs. Recently, a laboratory experiment was conducted to investigate both the behavior of a viscous, multicomponent NAPL in a fluctuating water table system and its subsequent dissolution (Figure 2). The experimental

work builds on the multifluid flow theory developed by Oostrom and Lenhard (2003) and Oostrom et al. (2003).

With respect to the movement of viscous NAPL, EMSL flow cell experiments have shown that the viscosity differences between the water and the light-NAPL are likely to result in entrapment of continuous oil lenses beneath the groundwater table. During this first part of the experiment, a two-dimensional container was packed with sands resembling those which occur in the underground at the Hanford site. Initially, the groundwater was maintained at such a level that the top part of the porous medium was partly saturated. Then a NAPL consisting of DBBP, TBP, and lard oil components was introduced and allowed to redistribute. After static equilibrium was reached, quantitative measurements of NAPL saturations were obtained using EMSL's newly constructed state-of-the-art dual-energy gamma radiation system (Figure 3). Subsequently, the groundwater table was lowered in several steps, until a minimum level was reached, followed by gradual incremental increases of the water table. After the original water level was reached, the NAPL was allowed to come to static equilibrium. At that point, the container was scanned again using the gamma system.



Figure 3. EMSL's newly constructed state-of-the-art dual-energy gamma radiation system was used to quantitatively measure NAPL saturations.

In the second part of the experiment, the mass transfer between the multicomponent NAPL source area and the ambient groundwater was investigated by imposing a horizontal groundwater flow in the container. At regular intervals, groundwater samples were extracted from sample ports in the flow cell and analyzed for dissolved organics. The resulting time series of aqueous phase concentrations allowed insight to the emission of organic solutes from the source area, which is expected to consist of a combination of discontinuous NAPL droplets and continuous oil lenses. Because a multicomponent light-NAPL was used, a study was performed of preferential dissolution of the more water soluble component and the resulting weathering processes of both the oil lens and the discontinuous oil droplets.

Quantitative data obtained during both phases of this experiment will be used to validate two numerical codes: STOMP and Modelcode Olie, a TNO-NITG simulator.

Citations

Oostrom M, and RJ Lenhard. 2003. "Carbon Tetrachloride Flow Behavior in Unsaturated Hanford Caliche Material: An Investigation of Residual Nonaqueous Phase Liquids." *Vadose Zone Journal* 2(1):25-33.

Oostrom M, C Hofstee, RJ Lenhard, and TW Wietsma. 2003. "Flow Behavior and Residual Saturation Formation of Liquid Carbon Tetrachloride in Unsaturated Heterogeneous Porous Media." *Journal of Contaminant Hydrology* 64(1-2):93-112.

The Binding Energies of Isomers of Water Clusters: High-Level Electronic Structure and Empirical Potential Results

SS Xantheas,^(a) GS Fanourgakis,^(a) and E Aprà^(b)

(a) Pacific Northwest National Laboratory, Richland, Washington

(b) W.R. Wiley Environmental Molecular Sciences Laboratory, Richland, Washington

The structures and energetics of water clusters play an important role in quantifying the interactions among water molecules. This molecular-level information assists in the development of empirical models used to study condensed phases such as liquid water and ice and to examine the transitions between the two phases.

In this work, the MP2 complete basis set (CBS) limit for the binding energy of the two low-lying water octamer isomers of D_{2d} and S_4 symmetry (Figure 4) is estimated at -72.7 ± 0.4 kcal/mol using the family of augmented correlation-consistent orbital basis sets of double through quintuple zeta quality. The largest MP2 calculation with the augmented quintuple zeta (aug-cc-pV5Z) basis set—2296 contracted gaussian basis functions—produced binding energies of -73.70 (D_{2d}) and -73.67 kcal/mol (S_4). The effects of higher correlation, computed at the CCSD(T) level of theory, are estimated at <0.1 kcal/mol (Xantheas and Aprà 2004).

The newly established MP2/CBS limit for the water octamer is reproduced quite accurately by the newly developed all-atom polarizable, flexible interaction potential (TTM2-F) (Burnham and Xantheas 2002). The TTM2-F binding energies of -73.21 (D_{2d}) and -73.24 kcal/mol (S_4) for the two isomers are just 0.5 kcal/mol (or 0.7%) larger than the MP2/CBS limit (Figure 5).

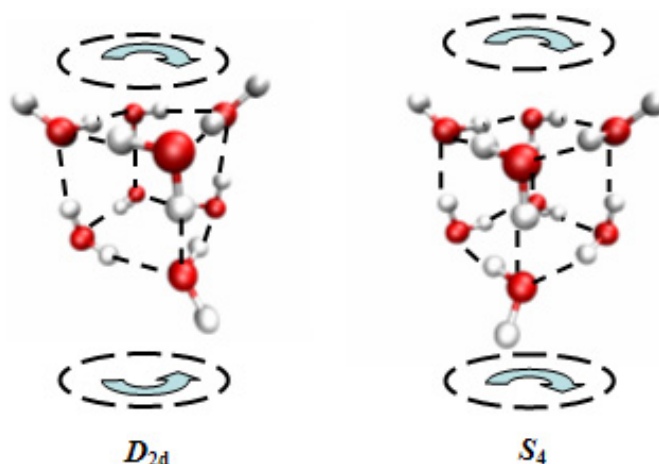


Figure 4. Structures of the D_{2d} and S_4 water octamer isomers showing the direction of the in-the-ring hydrogen bonded networks of the two constituent tetramers.

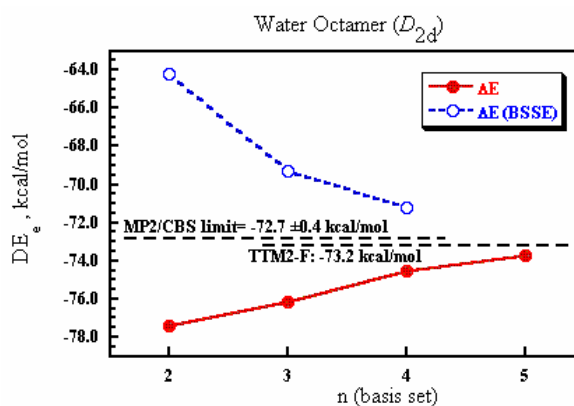


Figure 5. Variation of the uncorrected (solid circles) and BSSE-corrected (open circles) binding energy with basis set for the D_{2d} isomer of the water octamer.

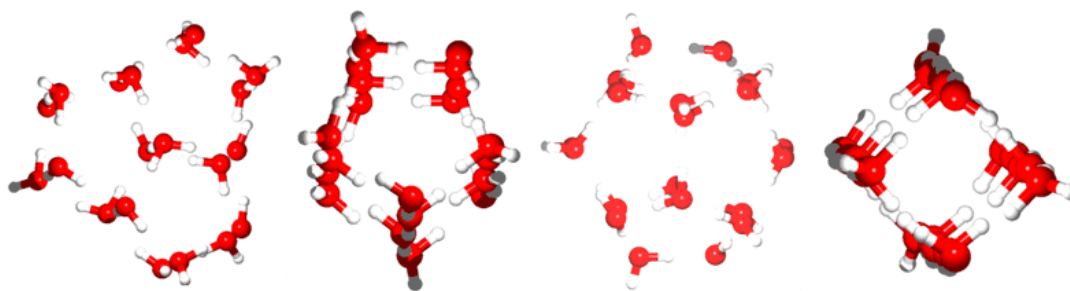


Figure 6. Isomers of the $(\text{H}_2\text{O})_{20}$ water cluster: edge-sharing, face-sharing, dodecahedron, and box-kite.

A similar theoretical approach has been used to study the larger $(\text{H}_2\text{O})_{20}$ water clusters. Extensive MP2 calculations have been used to accurately determine the most stable isomer (the edge-sharing isomer shown in Figure 6), compute binding energies (that once again were matched by the results of the TTM2-F potential), and generate vibrational frequencies that will be compared with experimental spectra.

The largest MP2 calculation for these series of molecules was performed with the aug-cc-pVQZ basis set, for a total of 3440 basis functions. The computational requirements of this calculation required current state-of-the-art in both electronic software and hardware.

All MP2 calculations were carried out using the NWChem (Kendall et al. 2000) code on the newly acquired supercomputer at the EMSL Molecular Science Computing Facility.

Citations

Burnham CJ and SS Xantheas. 2002. "Development of Transferable Interaction Models for Water: IV. A Flexible, All-Atom Polarizable Potential (TTM2-F) Based on Geometry Dependent Charges Derived from an *ab initio* Monomer Dipole Moment Surface." *Journal of Chemical Physics* 116(12):5115-5124.

Kendall RA, E Aprà, DE Bernholdt, EJ Bylaska, M Dupuis, GI Fann, RJ Harrison, J Ju, JA Nichols, J Nieplocha, TP Straatsma, TL Windus, and AT Wong. 2000. "High Performance Computational Chemistry: An Overview of NWChem a Distributed Parallel Application." *Computer Physics Communications* 128(1-2):260-283.

Xantheas SS and E Aprà. 2004. "The Binding Energies of the D_{2d} and S_4 Water Octamer Isomers: High-Level Electronic Structure and Empirical Potential Results." *Journal of Chemical Physics* 120(2):823-828.

Reliable Electronic Structure Calculations for Heavy Element Chemistry: Molecules Containing Actinides, Lanthanides, and Transition Metals

BE Bursten,^(a) LJ Sonnenberg,^(a) EJ Palmer,^(a) T Yang,^(a) MM Marino,^(b) W Ermler,^(b) C Zhan,^(c) K Hirao,^(d) IA Infante,^(e) DA Dixon,^(f) BP Hay,^(f) TK Firman,^(f) Z Zhang,^(g) RJ Harrison,^(h) L Visscher,⁽ⁱ⁾ SJ Van Gisbergen,⁽ⁱ⁾ WA de Jong,^(j) J Li,^(j) KG Dylla,^(k) PS Bagus,^(l) AK Wilson,^(l) S Matsika,^(m) J Autschbach,⁽ⁿ⁾ and B LeGuennic⁽ⁿ⁾

(a) Ohio State University, Columbus, Ohio

(b) University of Memphis, Memphis, Tennessee

(c) University of Kentucky, Lexington, Kentucky

(d) University of Tokyo, Tokyo, Japan

(e) Universiteit Amsterdam, Amsterdam, The Netherlands

(f) Pacific Northwest National Laboratory, Richland, Washington

(g) Lawrence Berkeley National Laboratory, Berkeley, California

(h) Oak Ridge National Laboratory, Oak Ridge, Tennessee

(i) Vrije Universiteit, Amsterdam, The Netherlands

(j) W.R. Wiley Environmental Molecular Sciences Laboratory, Richland, Washington

(k) Independent Researcher, Portland, Oregon

(l) University of North Texas, Denton, Texas

(m) Temple University, Philadelphia, Pennsylvania

(n) State University of New York, Buffalo, New York

The goal of this research is to study the chemistry of heavy elements through the use of *ab initio* electronic structure calculations, in order to improve the understanding of the behavior of actinides, lanthanides, and heavy transition metals—molecules critical to DOE missions such as environmental remediation.

During the first two years of this project, a wide variety of quantum chemical methods, based on molecular orbital theory and density functional theory with the proper treatment of relativistic effects, were used to interpret experimental data and predict the chemistry of actinide, lanthanide, and transition metal compounds. The results provided a firm theoretical basis for this area of chemistry, extending expensive experimental results into new areas of parameter space. The information obtained from calculations on actinide-containing molecules includes, but is not limited to, molecular structure, spectroscopic properties (infrared, NMR, ultraviolet-vis, ESR), complexation binding energies, and redox chemistry. The results of the calculations help enable the characterization of the interaction of the actinide, lanthanide, and heavy transition metal ions with organic complexing agents present in nuclear processing waste tanks and with anion ligands present in natural aqueous systems (e.g., carbonates). This work is leading to a better understanding of the fate and transport of actinides in the environment and of their interactions with new complexants such as phosphates and amides, in turn leading to the design of new innovative *in situ* remediation technologies and novel separation systems. The results obtained from the calculations are an invaluable supplement to current, very expensive experimental studies of the radioactive actinides, lanthanides, and radioactive heavy transition metal elements, allowing limited

experimental data to be extrapolated to many other regimes of interest.

The radioactive actinide elements americium and curium are chemically similar to their lanthanide counterparts. Both are present in nuclear wastes and thus present a challenge for actinide separation. Organodithiophosphinates (Figure 7, middle) have great selectivity for americium over the lanthanide elements. Calculations are used to analyze the structural differences in americium-complexation relative to the lanthanides. This difference has been observed experimentally and suggested as the basis for this selectivity. Another compound

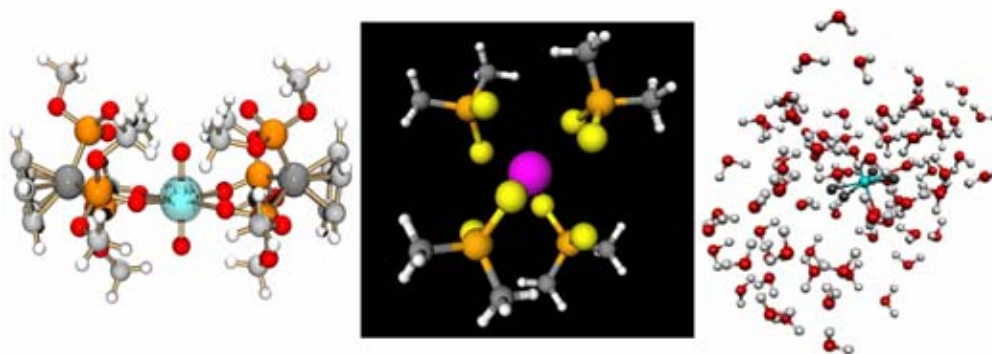


Figure 7. Some molecular actinide systems studied in this project: Uranyl binding with two Kläui ligands (left), americium binding to organodithiophosphate derivatives (middle), and uranyl fluoride molecule solvated in water (right).

with a potential application in actinide separation chemistry is the Kläui ligand, currently being studied experimentally at PNNL. The calculations provide insight into the binding ability of various derivatives of these ligands, for example the binding of one or two Kläui ligands with uranyl (Figure 7, left), uranium, and thorium, to guide the design of new and better separation agents.

Understanding the potential reactions of uranyl (UO_2^{2+}) and carbon tetrachloride is critical for the remediation of radioactive wastes at the Hanford Site. The calculations are focused on determining the solvent phase energetics to provide the data for reliable fate and transport models for uranyl species. Similar studies were performed on the formation and solvation of uranyl halides (Figure 7, right) and various other actinide-water complexes.

Experiments performed at the University of Virginia, and the calculations on CUO molecules in noble gas (argon and neon) matrices led to the discovery of actinide-noble gas complexes (Li et al. 2002). Another combined computational/experimental effort is the development of NMR as a tool for determining the speciation of nuclear waste in the Hanford tanks. The calculations of the NMR properties of uranyl carbonate and nitrate crystals predicted record-wide signals for the uranium-bonded oxygen atoms, subsequently confirmed by experiments at PNNL.

Citation

Li J, BE Bursten, B Liang, and L Andrews. 2002. "Noble Gas-Actinide Compounds: Complexation of the CUO Molecule by Ar, Kr, and Xe Atoms in Noble Gas Matrices." *Science* 295(5563):2242-2245.

Ionization Energy Calculations on Deoxyribonucleotides

ER Vorpagel^(a) and X Wang^(b)

(a) W.R. Environmental Molecular Sciences Laboratory, Richland, Washington

(b) Pacific Northwest National Laboratory, Richland, Washington

The goal of this research is to provide computational insight into the vertical electron detachment energy spectrum (VDE) measured experimentally.

Gas-phase electron binding energies for 2'-deoxyribonucleotides (dAMP-, dCMP-, dGMP-, dTMP-, and dUMP-) were measured using photo-detachment photoelectron spectroscopy and electrospray ionization. The VDE spectra were very broad, with the exception that dGMP had a small peak at a lower energy. Ion mobility experiments indicated only one conformation is present. Molecular mechanics calculations had been used to identify low energy conformations for these structures and were used as initial structures for density functional theory calculations using B3LYP and a TZVP+ basis set.

The NWChem software was run on MSCF resources with the help of Ecce software to search for the global minimum energy conformation for each anion. VDE was calculated for several conformations. Table 1 shows good agreement between theory and experiment for the lowest energy conformation.

The dGMP anion has a particularly good internal hydrogen bond that forms between the 6-amino group on the guanine base and one of the phosphate oxygen atoms. This causes the unexpectedly low VDE. Higher energy conformations of the dGMP anion without the extra hydrogen bond have higher calculated VDE values around 5.2 eV.

Figure 8 shows the highest occupied molecular orbital (HOMO) from which the electron is removed in the experiment. For the dGMP anion, the HOMO is located on the guanine base, whereas for the other standard DNA bases, the HOMO is on the phosphate groups.

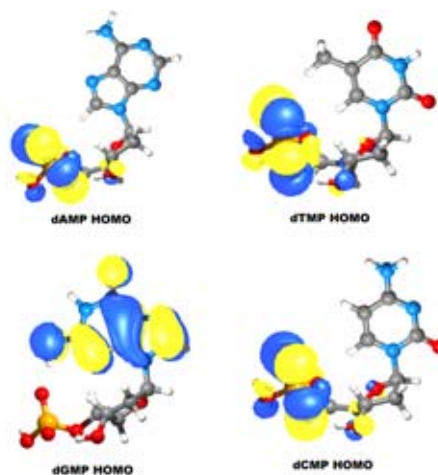


Figure 8. The HOMO from which the electron is removed in the experiment.

Table 1. VDE calculations.		
Molecule	VDE(exp)	VDE(calc)
dGMP	4.90 ± 0.1	4.90 eV
dTMP	5.80 ± 0.1	5.36 eV
dAMP	6.05 ± 0.1	5.23 eV
dCMP	5.80 ± 0.1	5.24 eV
dUMP	5.80 ± 0.1	5.50 eV

Selective Formation of Single-Phase Oxide Nanoclusters: Cu_2O on $\text{SrTiO}_3(100)$

IV Lyubinetsky,^(a) S Thevuthasan,^(a) and DR Baer^(b)

(a) W.R. Wiley Environmental Molecular Sciences Laboratory, Richland, Washington

(b) Pacific Northwest National Laboratory, Richland, Washington

Synthesis of three-dimensional nanostructures, such as nanoclusters of metals and semiconductors, results in formation of quantum dots possessing novel electronic and optical properties derived from the quantum confinement of charge carriers. Nanoscaled clusters also attract interest with respect to phase transitions, which may be different from those observed in bulk due to the increase of the surface-to-bulk ratio. Oxides constitute a highly diverse class of materials with rich optical, electronic, magnetic, and dielectric properties, and as such, have significant technological potential. Cuprous oxide (Cu_2O) is of considerable interest due to its unique electronic structure, and also is evolving in potential in chemical and photochemical applications, in particular, water splitting. Oxides physical and chemical properties are closely related to their crystalline quality, structure, and stoichiometry. Copper oxides are known to crystallize in two different phases:

Cu_2O (cuprous) and CuO (cupric oxide). Experimental parameters were evaluated for the formation of the single phase Cu_2O nanoclusters on the $\text{SrTiO}_3(001)$ surface in terms of the pressure-temperature phase diagram. The copper oxide nanoclusters were synthesized using oxygen plasma-assisted molecular beam epitaxy. The chemical state information from the surface region of the nanoclusters was acquired using *in-situ* x-ray photoelectron spectroscopy (XPS) and x-ray induced Auger electron spectroscopy (AES). *Ex-situ* analysis involved use of an atomic force microscope to map the morphology of the clusters.

Since copper has multiple oxidation states, the chemical state of the synthesized nanoclusters should be verified. Figures 9a and b present the $\text{Cu } 2p_{3/2}$ core level x-ray photoelectron and Auger $\text{Cu } L_3VV$ spectra, respectively, from samples containing copper in all three different charge states. The $2p$ peak binding energy difference between Cu^{2+} and Cu^{1+} (in Cu_2O) is quite large ($\Delta E \sim 1.6$ eV) and can be clearly resolved in a XPS spectrum containing a mixture of Cu^{1+} and Cu^{2+} (Figure 9a). Meanwhile, it is difficult to resolve the peaks due to Cu^0 and Cu^{1+} in XPS spectra. Cu and Cu_2O Auger peaks are well separated in AES, as shown in

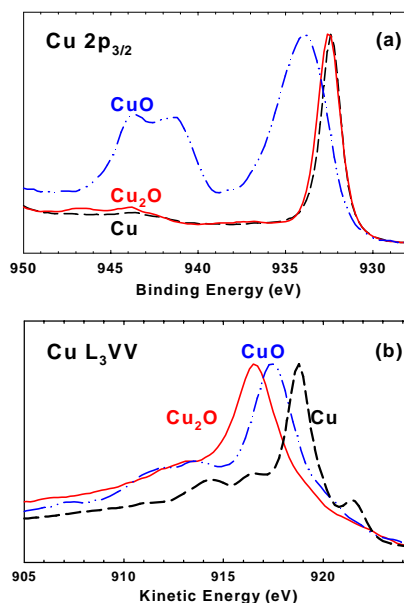


Figure 9. XPS $\text{Cu } 2p_{3/2}$ (a) and AES $\text{Cu } L_3VV$ (b) spectra of CuO , Cu_2O , and Cu .

Figure 9b, where the major Cu L₃VV Auger peaks associated with Cu⁰ and Cu¹⁺ have kinetic energies of 918.8 and 916.4 eV, respectively. Analyzing the experimental parameters for the Cu₂O nanoclusters formation, a phase diagram as a function of growth temperature and oxygen pressure under constant Cu flux has been determined and is shown in Figure 10. For comparison purposes, Figure 10 also displays the bulk Cu-O phase diagram. It is remarkable that a region associated with the growth of pure Cu₂O nanoclusters is observed to be very narrow, especially if compared to the bulk Cu-O phase diagram, making it quite a challenge to achieve the formation of the nanodots containing a single phase of cuprous oxide. In the studied temperature range of 450 to 850°C, the corresponding oxygen pressure region covers just less than the order of magnitude for nanoclusters versus more than six orders for bulk Cu₂O. Another notable observation is two distinctive mixed phase bands in phase space for the nanoclusters. The band observed at higher oxygen pressure than required for pure Cu₂O growth (Figure 10) contains Cu in two different charge states of Cu¹⁺ and Cu²⁺, while Cu¹⁺ and Cu⁰ observed in second band at lower pressures. It is considerably different from the bulk, that outside the fine Cu₂O region in phase diagram for the nanoclusters, there are the bands of temperature and pressure, within which two phase-like forms coexist, not as the rather sharp phase boundaries observed for the bulk. This may be considered as the experimental confirmation of the theoretical prediction of the multiphase coexistence bands for the small systems, which is the consequence of the small differences between the free energies of clusters in different phase-like forms. In principle, this should be also observed for other multicomponent nanoclusters containing components, which exhibit multiple charge states.

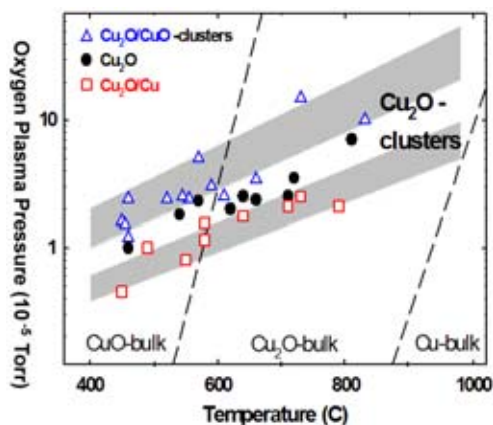


Figure 10. Phase diagram for the formation of the copper oxide nanoclusters on SrTiO₃.

Formation of nanoclusters on SrTiO₃(100) has been observed at all growth parameters studied, but structural details have been found to depend on the island composition. For the same amount of deposited Cu, Figures 11a, b, and c illustrate the typical morphologies observed for different regions of the phase diagram. For the pure Cu₂O (Figure 11a), morphology consists of isolated small (20- to 50-nm lateral dimensions) square/rectangular clusters with flat tops, and oriented mostly along the same <100> direction, indicating a crystalline ordering and epitaxy. For Cu₂O/CuO region (Figure 11b), there is a coexistence of the similar small, and the large (100 to 150 nm) more round shaped clusters, indicating possible phase-like separation for the cuprous and cupric oxides. In contrast, there are only minor changes in the morphology for the Cu₂O/Cu region, in particular (Figure 11c), a slight reduction of the square cluster size (10 to 40 nm) with simultaneous increase of quantum dot density.

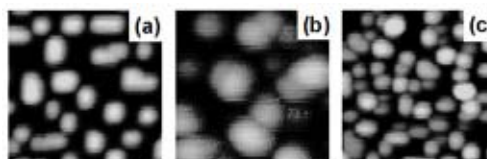


Figure 11. AFM 300 nm × 300 nm × 20 nm images for nano-clusters grown at 600°C at oxygen pressure of (a) 1.5 × 10⁻⁵, (b) 3.5 × 10⁻⁵, (c) 9.0 × 10⁻⁶ Torr.

In summary, selective formation of the single-phase nanoclusters of Cu_2O on $\text{SrTiO}_3(100)$ substrates in the size range of 10 to 50 nm is found to occur only in a very narrow oxygen plasma-assisted molecular beam epitaxy growth parameter window, in comparison with the bulk phase diagram (for oxygen pressure vs. temperature). There are distinctive parameter regions, where multiple phase-like forms coexist ($\text{CuO}/\text{Cu}_2\text{O}$ and $\text{Cu}_2\text{O}/\text{Cu}$), in agreement with theoretical prediction for small systems, and as opposite to the sharp phase boundaries for the bulk. Observed changes in the nanocluster composition are found to correlate with differences in cluster morphologies.

Oxygen Analysis Using Ion Beam Methods

W Jiang,^(a) V Shutthanandan,^(b) S Thevuthasan,^(b) DE McCready,^(b) and WJ Weber^(a)

(a) Pacific Northwest National Laboratory, Richland, Washington

(b) W.R. Wiley Environmental Molecular Sciences Laboratory, Richland, Washington

Nuclear reaction analysis (NRA) complements the widely used Rutherford backscattering spectrometry and is the preferred method for analyzing light elements on or near the surface of compound-containing heavy elements. There are many prominent features of NRA, including high selectivity of isotopes, good sensitivity for many nuclides, non-destructive depth profiling, and quantitative analysis of elemental concentrations. Using a thin amorphous layer of SiO_2 ($5.2 \mu\text{g}/\text{cm}^2$) on silicon, cross sections for the nuclear reactions $^{16}\text{O}(\text{d},\text{p}_1)^{17}\text{O}$, $^{16}\text{O}(\text{d},\alpha)^{14}\text{N}$ and $^{16}\text{O}(\alpha,\alpha)^{16}\text{O}$ at a laboratory angle of 150 degrees are determined over energies ranging from 0.701 to 1.057 MeV for D^+ ions and from 2.949 to 3.049 MeV for He^+ ions.

Based on a calibration of the thickness-corrected data using a reference point of 4.42 mb/sr at $E_d = 0.886$ MeV and $\theta_{\text{Lab}} = 150$ degrees, the absolute values of the cross section for the

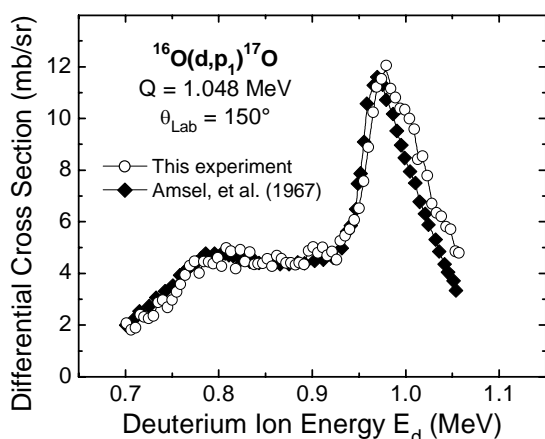


Figure 12. Cross sections for the reaction $^{16}\text{O}(\text{d},\text{p}_1)^{17}\text{O}$ at 150 degrees as a function of ion energy. Also included are the data at the same reaction angle (Amsel et al. 1967).

$^{16}\text{O}(\text{d},\text{p}_1)$ reaction were obtained, which are shown in Figure 12 as a function of the primary D^+ energy E_d . Also included in the figure are results (Amsel et al. 1967) for the excitation curve at $\theta_{\text{Lab}} = 150$ degrees. In general, there is an excellent agreement between the two data sets. This confirms the previous results and validates the current measurement. The total experimental error for the cross section data was estimated to be on the order of 4%. From Figure 12, there is a monotonic increase of the cross section with increasing D^+ energy from 0.701 to 0.774 MeV. A plateau-like structure appears between 0.774 and 0.926 MeV

on the excitation curve. The average value of the cross section in this energy range corresponds to 4.56 mb/sr with a fluctuation of $\sim 10\%$. From 0.926 MeV to 1.057 MeV, there is a broad resonant peak with the maximum intensity of ~ 12.1 mb/sr at 0.979 MeV and a full width at half maximum (FWHM) of 95 keV. Although the cross section value is relatively small, the plateau can be used for analysis of ^{16}O in materials. The energy width (152 keV) of the plateau corresponds to a detectable depth of over 1 μm for most oxide materials, such as SrTiO_3 , based on the SRIM2000 database. For conventional ion-beam analysis using a surface-barrier detector, this cross section plateau is not strongly recommended for profiling ^{16}O , as the depth resolution is poor, on the order of 100 nm.

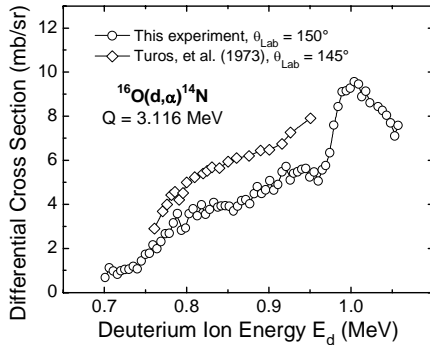


Figure 13. Cross sections for the reaction $^{16}\text{O}(\text{d},\alpha)^{14}\text{N}$ at 150 degrees as a function of ion energy. Also included are the data at $\theta_{\text{Lab}} = 145$ degrees (Turos et al. 1973).

notable difference is in the absolute values of the differential cross sections at 145 degrees, which are 20 to 35% larger. The difference could be attributed partly to data calibration that was not discussed in that report. The result from this study also shows a broad resonance that appears between 0.96 and 1.06 MeV with the maximum cross section of 9.56 mb/sr at 1.004 MeV. Since the cross section of the $^{16}\text{O}(\text{d},\alpha)$ reaction varies slowly with ion energy between 0.8 and 0.9 MeV, it has been used for depth profiling of oxygen in SiO_2 layers up to 600 nm in depth.

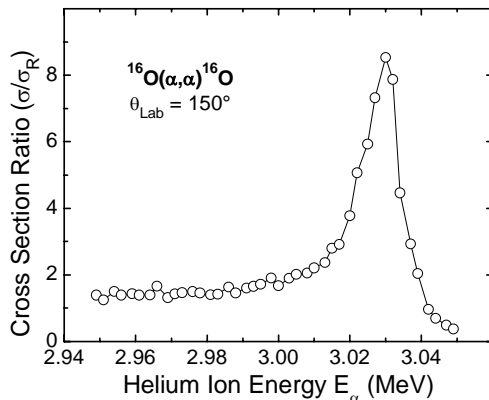


Figure 14. Cross sections for the scattering $^{16}\text{O}(\alpha,\alpha)^{16}\text{O}$ at 150 degrees as a function of ion energy.

Figure 13 shows the excitation curve from this study for the reaction $^{16}\text{O}(\text{d},\alpha)^{14}\text{N}$ at $\theta_{\text{Lab}} = 150$ degrees over energies ranging from 0.701 to 1.057 MeV. The thickness-corrected relative cross sections were normalized for 5.07 mb/sr at $E_d = 0.901$ MeV. This calibration is based on the average value of the cross sections of 4.40 mb/sr at 135 degrees and 5.75 mb/sr at 165 degrees, since there is no data available at 150 degrees for the reaction. Also included in Figure 12 is the reported data at $\theta_{\text{Lab}} = 145$ degrees from 0.750 to 0.950 MeV. In general, both curves show an increase in cross sections with increasing ion energy over the energy range, and the rates of increase are comparable. The most

For He^+ elastic scattering from ^{16}O , the cross section data for $\theta_{\text{Lab}} = 150$ degrees are plotted in Figure 14. There is only a gradual increase over the energy range from 2.95 to 3.01 MeV, followed by a sharp nuclear resonant peak at 3.030 ± 0.005 MeV (with a FWHM of ~ 12 keV). The maximum cross section at the peak corresponds to $8.54\sigma_R$. Previous investigations have determined the peak maximum values of $14.4\sigma_R$ at 165 degrees and of $22.7\sigma_R$ at 170.5 degrees. This indicates that there is a strong angular dependence of the nuclear resonance, and the peak cross section

increases rapidly with increasing scattering angle. This strong, narrow, and isolated nuclear resonance of $^{16}\text{O}(\alpha,\alpha)$ is recommended for depth profiling of ^{16}O . Based on the FWHM of the peak, the depth resolution corresponds to 34 and 48 nm for ^{16}O analysis in the near-surface region of SrTiO_3 and SiO_2 , respectively.

Five data sets of the measured cross sections for oxygen analysis have been tabulated, and a typical example has been given in Jiang et al. (2003).

Citations

Amsel G and D Samuel. 1967. "Microanalysis of the Stable Isotopes of Oxygen by Means of Nuclear Reactions." *Analytical Chemistry* 39:1689-1698.

Jiang W, V Shutthanandan, S Thevuthasan, DE McCready, and WJ Weber. 2003. "Oxygen Analysis Using Energetic Ion Beams." *Nuclear Instruments and Methods in Physics Research B* 207(4):453-461.

Turos A, L Wielunski, and A Barcz. 1973. "Use of the $\text{O }^{16}\text{O}(\text{d},\alpha)^{14}\text{N}$ Nuclear Reaction in the Microanalysis of Oxide Surface Layers." *Nuclear Instruments and Methods* 111:605-610.

ν_3 and $2\nu_3$ Bands of $^{32}\text{S}^{16}\text{O}_3$, $^{32}\text{S}^{18}\text{O}_3$, $^{34}\text{S}^{16}\text{O}_3$, and $^{34}\text{S}^{18}\text{O}_3$

SW Sharpe,^(a) TA Blake,^(b) RL Sams,^(a) A Maki,^(c) A Masiello,^(d) JB Barber,^(d)
N Vulpanovici,^(d) JW Nibler,^(d) and A Weber^(e)

(a) Pacific Northwest National Laboratory, Richland, Washington

(b) W.R. Wiley Environmental Molecular Sciences Laboratory, Richland, Washington

(c) Consultant, Mill Creek, Washington

(d) Oregon State University, Corvallis Oregon

(e) National Science Foundation, Arlington, Virginia, and the National Institute of Standards and Technology, Gaithersburg, Maryland

Historically, the spectroscopic and structural investigations of sulfur trioxide, SO_3 , have taken place in three stages. Beginning in the second half of the 1930s, vibrational Raman, infrared, and electron diffraction studies provided the first reliable information about the vibrational frequencies and structure of this molecule. Solid, liquid, and gas phase studies were undertaken that showed that the molecule exists principally as a monomer in the gas phase, but also as a trimer, S_3O_9 , especially in the liquid and solid states of aggregation. The monomer molecule was found to exist as a symmetric planar configuration described by the point group D_{3h} . The six vibrational degrees of freedom give rise to four fundamental frequencies. Using contemporary values for the frequencies, these describe the totally symmetric S–O stretching mode $\nu_1 = 1065 \text{ cm}^{-1}$, the non-degenerate out-of-plane bending vibration $\nu_2 = 498 \text{ cm}^{-1}$, the doubly degenerate antisymmetric in-plane S–O stretching vibration $\nu_3 = 1391 \text{ cm}^{-1}$, and the doubly degenerate in-plane bending with $\nu_4 = 530 \text{ cm}^{-1}$. For transitions from the ground state, the ν_1 mode is allowed only in Raman scattering, while the ν_2 mode is active as an infrared dipole transition only. The two degenerate vibrations ν_3 and ν_4 are allowed as both infrared and Raman transitions. The molecule possesses no permanent electric dipole moment that could give rise to a conventional pure rotational infrared or microwave spectrum.

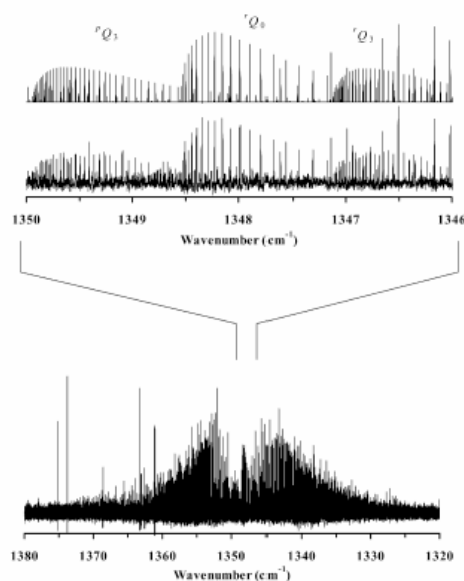


Figure 15. Overview of the Q-branch region of ν_3 of $^{32}\text{S}^{18}\text{O}_3$.

In this work, the high-resolution rotation–vibration spectra of sulfur trioxide is reported. We make a systematic study of the ν_3 and $2\nu_3$ infrared bands of the four symmetric top isotopomers $^{32}\text{S}^{16}\text{O}_3$, $^{32}\text{S}^{18}\text{O}_3$, $^{34}\text{S}^{16}\text{O}_3$, and $^{34}\text{S}^{18}\text{O}_3$. A sample spectrum is shown in Figure 15. The ground and upper state rotational constants as well as vibrational anharmonicity constants are reported. The constants for the center-of-mass substituted species $^{32}\text{S}^{16}\text{O}_3$ and $^{34}\text{S}^{16}\text{O}_3$ vary only slightly, as do the constants for the $^{32}\text{S}^{18}\text{O}_3$, $^{34}\text{S}^{18}\text{O}_3$ pair. The S–O bond lengths for the vibrational ground states of the species $^{32}\text{S}^{16}\text{O}_3$, $^{34}\text{S}^{16}\text{O}_3$, $^{32}\text{S}^{18}\text{O}_3$, and $^{34}\text{S}^{18}\text{O}_3$

are, respectively, 141.981 99(1), 141.979 38(6), 141.972 78(8), and 141.969 93(8) pm, where the uncertainties, given in parentheses, are two standard deviations and refer to the last digits of the associated quantity. Details of this work appear in Sharpe et al. (2003).

Citations

Sharpe SW, TA Blake, RL Sams, A Maki, A Masiello, J Barber, N Vulpanovici, JW Nibler, and A Weber. 2003. "The ν_3 and $2\nu_3$ bands of $^{32}\text{S}^{16}\text{O}_3$, $^{32}\text{S}^{18}\text{O}_3$, $^{34}\text{S}^{16}\text{O}_3$, and $^{34}\text{S}^{18}\text{O}_3$." *Journal of Molecular Spectroscopy* 222(2):142-152.

Awards and Recognition

Environmental Spectroscopy and Biogeochemistry Facility user and scientific consultant Kevin Rosso, PNNL, Richland, Washington, was the 2004 recipient of the Mineralogical Society of America Award (Figure 16). This award is one of the most prestigious awards in the entire field of geosciences and is given in recognition of outstanding published contributions to the science of mineralogy by individuals near the beginning of their professional careers. This award comes as a result of Rosso's contributions toward the development of a

fundamental understanding of the reactivity of mineral surfaces. An example is the experimental interrogation of the frontier molecular orbitals at FeS₂ pyrite surfaces using scanning tunneling spectroscopy, coupled with supporting *ab initio* calculations. This involved collection and physical interpretation of the first ever atomically-resolved scanning tunneling spectra acquired on mineral surfaces. Other examples include the introduction of a new theoretical model for calculating the kinetics of electron transfer reactions involving metal ions in aqueous solution, and also for contributions leading to the definition of the proximity effect on semiconducting mineral surfaces.

Gordon Anderson, Technical Leader of EMSL's Instrument Development Laboratory, was elected by the International Council on Systems Engineering as their 2003 Systems Engineer of the Year. Gordon was selected from a strong field of candidates and is recognized for his many contributions to improving systems engineering and implementation, including the electronics and data systems for the FTICR, a software analysis package for ion cyclotron resonance, a software package for use on the Snake and Columbia River dams to monitor juvenile salmon passage, and a small, portable battery-powered proportional counter for gamma and neutron signals. This work, coupled with his significant involvement over the past 15 years in educational programs to further science and engineering, made him an obvious choice for this award.

EMSL users and PNNL staff members Jean Futrell and Lai-Sheng Wang were recently elected as Fellows of the American Physical Society (APS). This is a very distinguished honor that is achieved by no more than one half of one percent of the APS membership. Both individuals, along with the other newly elected Fellows, will be featured in the March 2004 issue of *APS News*.

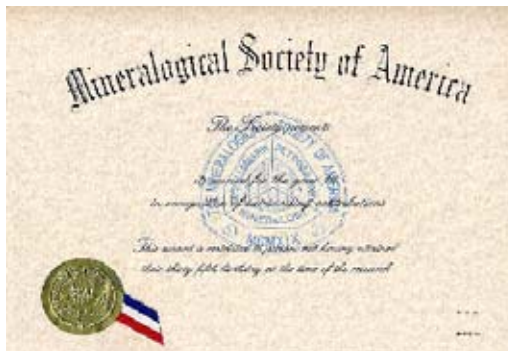


Figure 16. The Mineralogical Society of America Award.

Professional/Community Service

PNNL's research exhibit booth at Supercomputing 2003 (held in Phoenix, Arizona on November 17-20, 2003) was located at the entrance to the DOE section of the exhibit hall (Figure 17). The theme was "Science for Crossing Scales from Molecules to Mankind." Research in computational simulations, scalable tools, methods, and applications was highlighted. At the time of the event, EMSL's recently installed Linux-based,

massively parallel supercomputer from Hewlett Packard was rated the fifth fastest in the world. PNNL's exhibit provided information and demonstrations of current advances in computer science, applied math, and scalable simulation methods that are leading to solutions for DOE simulation challenges and other complex missions. Attendance at the conference was the largest ever both in attendees and in the number of exhibit booths. PNNL also participated in SciNet (a high-performance network built to support the annual event) by sending six people to build and maintain it, and the Student Day Career Fair, which provided an opportunity for students to learn about the research and mission of PNNL.



Figure 17. The view of PNNL's research booth as seen from the entrance into the exhibit hall. Looping videos were displayed on the monitors while demos were given at the corner computers.

Major Facility Upgrades

The new QsNet II network was installed on EMSL's supercomputer (HPCS2) and test jobs conducted. Much improvement was noted in code performance using this new network.

The availability of HPCS2 for production workload has been high, with many jobs consistently waiting in the queue. As large jobs await processors, nodes consistently become available for a short time. A computing grid has been implemented to take advantage of these unused cycles; a separate queue was built that allows lower priority jobs to use unused computing time. These jobs are then preempted as nodes are allocated to production jobs. This process allows more than 99% use of the system without impacting normal workload.

Preliminary design work on the MSCF expansion continued through November and early December. It was determined that 1 megawatt of power would be required for the new expansion. Half of this power would be backed by a UPS system instead of a generator. Formal design work will begin in January, with construction to be completed in Fiscal Year 2005.

News Coverage

PNNL's supercomputer was ranked fifth in the world according to the Top 500 list, and the resulting news release issued by PNNL and Hewlett Packard (HP) led to coverage in Computerworld, InformationWeek, IDG, MacWorld, and others.

The 11.8 teraflop supercomputer consists of nearly 2,000 1.5GHz Intel® Itanium®-2 processors, and this list represents the first time the system was ranked, based on its full power. The Top 500 list ranks computers based on their performance running a benchmark called Linpack, which is a method to measure a machine's ability to solve a set of dense linear equations.

The HP supercomputer is installed in the Molecular Science Computing Facility of the William R. Wiley Environmental Molecular Sciences Laboratory and is tailored to the requirements of large-scale computational, biological and chemical sciences. Large blocks of computing time are granted to multi-institutional research teams on a competitive proposal basis.

Visitors and Users

Chemistry and Physics of Complex Systems Facility

- Jenny Hand, Colorado State University, Fort Collins, Colorado, collaborated with Alex Laskin, W.R. Wiley Environmental Molecular Sciences Laboratory, Richland, Washington, on the study “Single Particle Analysis of Smoke Aerosols During the Yosemite Aerosol Characterization Study During Summer 2002.”
- Chris Manning, Manning Applied Technology, Troy, Idaho, presented the seminar “Extreme Interferometry.”

Environmental Spectroscopy and Biogeochemistry Facility

- Barry Bickmore, Brigham Young University, Provo Utah, in collaboration with Kevin Rosso, Pacific Northwest National Laboratory, Richland, Washington, worked on developing a new model for predicting acidity constants of molecules in aqueous solution using ab initio molecular dynamics simulations. A series of small anions were geometry optimized in vacuum and compared with their simulated structure upon solvation in water at room temperature to determine how bond lengths are modified by the solvent. The modification can be used to better understand the distribution of acidity constants about a mean value for monomers possessing equivalent functional groups. The calculations are also providing a systematic series of accurate bond lengths for model calibration.
- Anna Cavinato and Richard Armand Tache, Eastern Oregon University, La Grande, Oregon, in collaboration with Alan Joly and Zheming Wang, Pacific Northwest National Laboratory, Richland, Washington, (Figure 18) conducted time-of-flight experiments on fluorophore-added intralipid suspensions to build a calibration for the scattering coefficients in turbid media.
- G.V. Gibbs, Virginia Polytechnic Institute, Blacksburg, Virginia, collaborated with Kevin Rosso to initiate a series of calculations for analyzing and correlating electron density distributions in silicates with their acid/base reactivity. Density functional theory geometry optimizations were performed on EMSL’s massively parallel supercomputer. By plotting the Laplacian of the electron density distribution, localized sites with high propensities for either electrophilic or nucleophilic attack are unveiled. The calculations were performed on a canonical set of large SiO₂ polymorph clusters. The locations of predicted reactive sites will be compared with those derived from simulations of hydroxyl or proton attachment on the clusters.



Figure 18. Richard Tache, Anna Cavinato, and Alan Joly.

- Cor Hofstee, Netherlands Institute of Applied Geosciences, Utrecht, The Netherlands, in collaboration with Mart Oostrom, Pacific Northwest National Laboratory, Richland, Washington, (Figure 19) and Tom Wietsma, W.R. Wiley Environmental Molecular Sciences Laboratory, Richland, Washington, performed the first experiments using EMSL's newly constructed state-of-the-art dual-energy gamma radiation system. Laboratory experiments were conducted to investigate both the behavior of a viscous, multicomponent nonaqueous phase liquid in a fluctuating water table system and its subsequent dissolution.



Figure 19. Cor Hofstee and Mart Oostrom.

- Nick Norberg, University of Washington, Seattle, Washington, in collaboration with Jim Amonette, Pacific Northwest National Laboratory, Richland, Washington, and Ravi Kukkadapu, W.R. Wiley Environmental Molecular Sciences Laboratory, Richland, Washington, (Figure 20) used electron paramagnetic resonance spectroscopy to study Mn(II)-doped ZnO quantum dot samples. Spectra were collected in Q-band using the multifrequency continuous-wave instrument. These spectra provide information about the ligand-field environment of the manganese ions in the ground state and are used to improve understanding of how Mn(II) and other divalent metals alter the electronic and magnetic properties of ZnO nanocrystals.



Figure 20. L-R: Ravi Kukkadapu, Nick Norberg, and Jim Amonette.

High-Field Magnetic Resonance Facility

- Cheryl Arrowsmith, University of Toronto, University Health Network, Toronto, Ontario, Canada, sent samples to be run on the 800-MHz and 500-MHz spectrometers for the study "Structural Proteomics: Annotating the Genome Using 3D Structure."
- Peter Brzovic, University of Washington, Seattle, Washington, used the 800-MHz spectrometer for the study "NMR Structural Investigations of BRCA1."
- Brian Cherry and Todd Alam, Sandia National Laboratories, Albuquerque, New Mexico, sent samples to be run on the 500-MHz wide bore spectrometer for the study "Investigating the Heterogeneity of Polymer Aging."
- Colin Fyfe and Celine Schneider, University of British Columbia, Vancouver, British Columbia, Canada, sent samples to be run on the 800-MHz spectrometer for the study "Structural Investigations of Solid Materials by High-Resolution Solid-State NMR at Very High Field."

- Evan Kantrowitz, Boston College, Chestnut Hill, Massachusetts, sent samples to be run on the 800-MHz spectrometer for the study “Probing the Mechanism of the Alkaline Phosphatase Reaction by ^{67}Zn and ^{25}Mg NMR.”
- Gaetano Montelione and James Aramini, Rutgers University, Piscataway, New Jersey, sent samples to be run on the 800-MHz and 500-MHz spectrometers for the study “Structural Genomics of Eukaryotic Model Organisms.”
- Gerard Parkin, Columbia University, New York, New York, sent samples to be run on the 800-MHz spectrometer for the study “Solid-State ^{67}Zn NMR of Synthetic Metalloprotein Models.”
- Susan Wallace, University of Vermont, Burlington, Vermont, sent samples to be run on the 500-MHz spectrometer for the study “Interaction of *Escherichia coli* Formamidopyrimidine-DNA Glycosylase (Fpg) with Damaged DNA Containing a 7, 8-Dihydro-8-oxoguanine Lesion.”

High-Performance Mass Spectrometry Facility

- Terry Beveridge, University of Guelph, Guelph, Ontario, Canada, participated in studies of protein determinations for the purified outer membrane and total membrane of *Geobacter sulfurreducens*. Heme-stained proteins from spots from a two-dimensional electrophoresis gel are also being analyzed for determination of cytochrome c proteins.
- In the study of *Shewanella oneidensis*, Jim Fredrickson, PNNL, Richland, Washington, participated in analyses of samples ranging from the comparison of cells grown under aerobic and anaerobic conditions to the comparison of protein expression profiles from wild-type and mutant cells. Most of these samples have been analyzed on the FTICR using a range of techniques available, including stable isotope labeling, membrane and cytosolic preparations, vesicle preparations, and global tryptic lysate preparation.
- Michael Gerald Katze, University of Washington, Seattle, Washington, worked on the study “Cellular Response to Hepatitis C Virus Infection: Global Quantitative Proteome AMT Tag Measurements of Cellular Protein Expression.” The samples provided were fractionated and an Accurate Mass Tag database was generated. Several liver biopsy samples were analyzed, and it was shown that the viral proteins can be detected in the liver samples, as well as several novel proteins.
- Sandra McCutchen-Maloney, Lawrence Livermore National Laboratory, has begun manuscript preparation for the robust and comprehensive proteomic analysis of *Yersinia pestis*. Data is currently being collected for the second stage of the project: The quantitation of protein expression using stable isotopes.
- Anil J. Patwardhan, University of California, San Francisco, San Francisco, California, sent samples for fractionation and labeling for the study “Identification and Relative

Expression of Membrane Proteins in Breast Cancer Cell Lines.” Data analysis is in progress for the fractionated samples and the labeled samples have yet to be analyzed.

- Daniel Sforza, University of California, Los Angeles, Los Angeles, California, participated in “Preliminary Work on the Proteomes of Brains and Dissected Brains Obtained from Control Mice and Treated Mice Simulating Parkinson’s Disease.” In this study, brain striatum samples from the control and each dose group were analyzed using conventional electrospray ionization-ion trap mass spectrometry. The data was analyzed by EMSL researchers and given to the collaborator. Several labeling experiments are planned for the striatum samples as well to attempt to obtain protein expression quantitation data.

Instrument Development Laboratory

- Steve Van Orden, Joe Meier, Christian Berg, and Chris Thompson of Bruker Daltronics, Billerica, Massachusetts, met with Instrument Development Laboratory and other PNNL staff. The Bruker CREDO involves the development of software for automated interpretation of FITCH mass spectra. This is a joint development project that will greatly benefit EMSL’s high-throughput proteomics processing pipeline. Development of this new software version will at least double EMSL’s data processing throughput and require a significant reduction in hardware investment.

Interfacial and Nanoscale Science Facility

- Mark Bussell and his students, Michelle Robinson, Marian Kennedy, Kathryn Layman, Daniel Van Wyk, and Melissa Pease characterized new novel catalytic materials synthesized at Western Washington University, Bellingham, Washington. They used the surface analysis instrumentation, x-ray diffraction facility, and the electron microscopy suite to characterize their materials.
- Gary Hansen, Thomas McCord and Karl Hibbits, University of Washington, Seattle, Washington, visited the accelerator facility to continue work to understand the chemistry in non-ice solar system analogue materials during MeV ion irradiation. Patricia Beauchamp, Jet Propulsion laboratory, Pasadena, California, also visited at the same time to collaborate with the scientists.
- Nicholas Norberg, University of Washington, Seattle, Washington, visited the molecular beam epitaxy laboratory to continue studies of ferromagnetic element doped TiO₂ nanocrystalline materials
- Bruce Sass, Battelle Columbus, Columbus, Ohio, visited the surface science laboratory to continue studies on the characterization of pressure-treated wood.

Molecular Science Computing Facility

- Alejandro (Alex) Aceves-Gaona, Washington State University-Tri-Cities, Richland, Washington, worked with John Miller, Pacific Northwest National Laboratory, Richland, Washington, (Figure 21) on molecular dynamics simulations of DNA containing damage products associated with radiation exposure. Using MPP2, Aceves-Gaona is simulating DNA oligonucleotides with multiple damage sites, which distinguish radiation-induced DNA damage from the isolated lesions that result from normal oxidative stress. Miller and Aceves-Gaona are supported by a grant from DOE's Low Dose Radiation Research Program to investigate health effects of ionizing radiation at occupational and environmental levels of exposure.
- 
- Figure 21.** Aceves-Gaona and Miller working in the MSCF Graphics & Visualization Lab.
- Al Geist, Oak Ridge National Laboratory, Oak Ridge, Tennessee, was recently granted an allocation on the large 11.8 teraflop computer to examine "A New Approach to Protein Folding by Reducing Dimensionality of Protein Conformational Space." The method they developed is particularly suited for parallel computers with a large number of processors, such as at EMSL's Molecular Science Computing Facility.
 - Galya Orr and Serdar Ozcelik, Pacific Northwest National Laboratory, Richland, Washington, met with Graphics & Visualization Laboratory staff to assemble molecular models for epidermal growth factor (EGFR) homodimerization and heterodimerization with HER2 to calculate distance distributions between possible locations of donor and acceptor dye molecules bonded to antibodies attached to EGFR and HER2. The models based on several crystal structures gave distance distributions that were consistent with those obtained from fluorescence resonance energy transfer data.

Molecular Sciences Software - New User Agreements with NWChem/Ecce

- Argonne National Laboratory, Argonne, Illinois
- BASF AG, Ludwigshafen, Germany
- Campus de la Universidad Autónoma de Madrid, Madrid, Spain
- Center of Molecular and Macromolecular Studies, Lodz, Poland
- CogniTech Corp, Salt Lake City, Utah
- ECOLE Polytechnique Federal de Lausanne, Lausanne, Switzerland
- Emory University, Atlanta, Georgia
- Hope College, Holland, Michigan
- Institute of Macromolecular, Saint Petersburg, Russia
- Kasetsart University, Bangkok, Thailand

- Korea Institute of Science and Technology Information, Daejeon, Korea
- Laboratoire de Photophysique et Photochimie des Composés de Métaux de Transition, Geneva, Switzerland
- Nankai University, Tianjin, China
- NiKem Research, Milan, Italy
- Novozymes, Bagsvaerd, Denmark
- Polytechnic University, Brooklyn, New York
- San Diego State University, San Diego, California
- Seoul National University, Seoul, Korea
- Universidad de Oviedo, Oviedo, Spain
- Universidad Técnica Federico Santa María, Valparaíso, Chile
- University of Arizona, Tucson, Arizona
- University of California, Davis, Davis, California
- University of Science and Technology of China, Hefei, Anhui, Peoples Republic of China
- University of Buffalo, State University of New York, Buffalo, New York
- University of Tsukuba, Tsukuba, Japan
- University of Western Ontario, London, Ontario, Canada
- US ARMY Corp of Engineers, Vicksburg, Mississippi
- Utah State University, Logan, Utah
- VTT Technical Research Centre of Finland, Tampere, Finland
- Yale University, New Haven, Connecticut

New EMSL Staff

Samina Azad was hired as a Limited Term Employee in the Interfacial and Nanoscale Science Facility group. She will be primarily responsible for the operation and maintenance of the Kratos Axis surface analytical instrumentation in collaboration with PNNL staff member Do Heui Kim.

Marisol Avila was hired as a part time staff member (Technician IV) in the Interfacial and Nanoscale Science Facility group. She will be primarily responsible for the operation and maintenance of the scanning electron microscope in collaboration with EMSL staff member Jim Young.

Publications

Amonette JE, SM Heald, and CK Russell. 2003. "Imaging the Heterogeneity of Mineral Surface Reactivity Using Ag(I) and Synchrotron X-ray Microscopy." *Physics and Chemistry of Minerals* 30(9):559-569.

Aramini JM, YJ Huang, JR Cort, S Goldsmith-Fischman, R Xiao, LY Shih, CK Ho, J Liu, B Rost, B Honig, MA Kennedy, TB Acton, and GT Montelione. 2003. "Solution NMR Structure of the 30S Ribosomal Protein S28E from *Pyrococcus Horikoshii*." *Protein Science* 12(12):2823-2830.

Barlow SE. 2003. "Alternative Electrostatic Green's Function for a Long Tube." *Journal of Applied Physics* 94(9):6221-6222.

Brinkman NR, and G Tschumper. 2003. "An Alternative Mechanism for the Dimerization of Formic Acid." *Journal of Physical Chemistry A* 107:10208-10216.

Fellows RJ, Z Wang, and CC Ainsworth. 2003. "Europium Uptake and Partitioning in Oat (*Avena sativa*) Roots as Studied By Laser-Induced Fluorescence Spectroscopy and Confocal Microscopy Profiling Technique." *Environmental Science and Technology* 37(22):5247-5253.

Gutsev GL, CW Bauschlicher, HJ Zhai, and LS Wang. 2003. "Structural and Electronic Properties of Iron Monoxide Clusters Fe_nO and Fe_nO ($n=2-6$): A Combined Photoelectron Spectroscopy and Density Functional Theory Study." *Journal of Chemical Physics* 119(21):11135-11145.

Hirata S. 2003. "Tensor contraction engine: a symbolic manipulation program for quantum-mechanical many-electron theories." *Journal of Chemical Physics A* 107:9887-9897.

Hirata S, CG Zhan, E Aprà, TL Windus, and DA Dixon. 2003. "A New, Self-Contained Asymptotic Correction Scheme to Exchange-Correlation Potentials for Time-Dependent Density Functional Theory." *Journal of Physical Chemistry A* 107(47):10154-10158.

Kukkadapu RK, JM Zachara, JK Fredrickson, SC Smith, AC Dohnalkova, and CK Russell. 2003. "Transformation of 2-Line Ferrihydrite to 6-Line Ferrihydrite Under Oxic and Anoxic Condition." *American Mineralogist* 88(11-12, Part 2):1903-1914.

Laskin J and JH Futrell. 2003. "Collisional Activation of Peptide Ions in FT-ICR Mass Spectrometry." *Mass Spectrometry Reviews* 22(3):158-181.

Neal AL, KM Rosso, GG Geesey, YA Gorby, and B Little. 2003. "Surface Structure Effects on Direct Reduction of Iron Oxides by *Shewanella oneidensis*." *Geochimica et Cosmochimica Acta* 67(23):4489-4503.

Rosso KM and ES Ilton. 2003. "Charge Transport in Micas: The Kinetics of $Fe^{II/III}$ Electron Transfer in the Octahedral Sheet." *Journal of Chemical Physics* 119(17):9207-9218.

Sharpe SW, TA Blake, RL Sams, A Maki, A Masiello, J Barber, N Vulpanovici, JW Nibler, and A Weber. 2003. "The ν_3 and $2\nu_3$ bands of $^{32}\text{S}^{16}\text{O}_3$, $^{32}\text{S}^{18}\text{O}_3$, $^{34}\text{S}^{16}\text{O}_3$, and $^{34}\text{S}^{18}\text{O}_3$." *Journal of Molecular Spectroscopy* 222(2):142-152.

Sugiki S, N Kurita, Y Sengoku, and H Sekino. 2003. "Fragment Molecular Orbital Method with Density Functional Theory and DIIS Convergence Acceleration." *Chemical Physics Letters* 382(5-6):611-617.

Wang X, S Niu, X Yang, SK Ibrahim, CJ Pickett, T Ichiye, and LS Wang. 2003. "Probing the Intrinsic Electronic Structure of the Cubane [4Fe-4S] Cluster: Nature's Favorite Cluster for Electron Transfer and Storage." *Journal of the American Chemical Society* 125(46):14072-14081.

Wind RA, JZ Hu, and DN Rommereim. 2003. "High-Resolution ^1H NMR Spectroscopy in a Live Mouse Subjected to 1.5 Hz Magic Angle Spinning." *Magnetic Resonance in Medicine* 50(6):1113-1119.

Wu B, A Yee, A Pineda-Lucena, A Semesi, TA Ramelot, JR Cort, JW Jung, A Edwards, W Lee, M Kennedy, and CH Arrowsmith. 2003. "Solution Structure of Ribosomal Protein S28E from *Methanobacterium Thermoautotrophicum*." *Protein Science* 12(12):2831-2837.

Xia Y, AR Felmy, L Rao, Z Wang, and NJ Hess. 2003. "Thermodynamic Model for the Solubility of ThO_2 (am) in the Aqueous Na^+ - H^+ - OH^- - NO_3^- - H_2O -EDTA System." *Radiochimica Acta* 91(12):751-760.

Zhai HJ, K Boggavarapu, J Li, and LS Wang. 2003. "Hydrocarbon Analogues of Boron Clusters--Planarity, Aromaticity, and Antiaromaticity." *Nature Materials* 2(12):827-833.

Zhai, HJ, LS Wang, AN Alexandrova, AI Boldyrev, and VG Zakrzewski. 2003. "Photoelectron Spectroscopy and *ab initio* Study of B_5^- and B_4^- Anions and Their Neutrals." *Journal of Physical Chemistry A* 107(44):9319-9328.

Presentations

Azad S, MH Engelhard, J Szanyi, and CHF Peden. 2003. "Adsorption and Reaction of NO and CO on $\text{CeO}_2(111)$ and $\text{Ce}_{0.8}\text{Zr}_{0.2}\text{O}_2(111)$ Surfaces." Presented by Samina Azad at the 50th American Vacuum Society International Symposium, Baltimore, Maryland, on November 3, 2003.

Azad S, S Thevuthasan, OA Marina, V Shutthanandan, LV Saraf, DE McCready, CM Wang, IV Lyubinetzky, and CHF Peden. 2003. "Influence of Multiple Interfaces on Oxygen Ionic Conductivity in Gadolinia-Doped Ceria and Zirconia Thin Films." Presented by Samina Azad at the 2003 Fall Materials Research Society Meeting, Boston, Massachusetts, on December 3, 2003.

Baer DR. 2003. "Metal Oxides, the Environment and Functional Nanostructures." Web presentation at MacDiarmid Institute Seminar involving seven Research Institutions, Dunedin, New Zealand, on November 21, 2003.

Buchko GW, S Ni, SR Holbrook, and MA Kennedy. 2003. "Solution Structure of the Hypothetical Nudix Hydrolase DR0079 from the Extremely Radiation-Resistant Bacterium *Deinococcus Radiodurans*." Presented by Michael A. Kennedy at the American Society for Microbiology Conference on DNA Repair & Mutagenesis, Kingston, on December 7, 2003.

Chambers SA, S Thevuthasan, TC Droubay, SM Heald, CM Wang, AS Lea, V Shutthanadan, J Osterwalder, YJ Kim, R Sears, B Taylor, and B Sinkovic. 2003. "MBE Growth and Properties of Fe-, Cr- and Mn-doped TiO₂ Rutile and Anatase." Presented by Scott Chambers at the 50th International American Vacuum Society Symposium, Baltimore, Maryland, on November 3, 2003.

Cooper DC, RK Kukkadapu, WA Smith, DT Fox, MA Plummer, and LC Hull. 2003. "Evidence for the Occurrence of Microbial Iron Reduction in Bulk Aerobic Unsaturated Sediments." Presented by D. Craig Cooper at the American Geophysical Union, San Francisco, California, on December 8, 2003.

Devanathan R, F Gao, and WJ Weber. 2003. "Molecular Dynamics Simulation of Point Defect Accumulation in ³C-SiC." Presented by Ram Devanathan at Proceedings of the 2003 Materials Research Society Fall Meeting, Boston, Massachusetts, on December 1, 2003.

Donley MS, LS Kasten, and DJ Gaspar. 2003. "Adhesion Chemistry of Self-Assembled Nano-phase Particle (SNAP) Treatments on Aluminum." Presented by Dan Gaspar at the American Vacuum Society's 50th International Symposium and Exhibition, Baltimore, Maryland, on November 5, 2003.

Droubay TC, TC Kaspar, CM Wang, and SA Chambers. 2003. "Ferromagnetic Co-Doped Anatase TiO₂: Are All Growth Methods Created Equal." Presented by Tim Droubay at the 50th International American Vacuum Society Symposium, Baltimore, Maryland, on November 3, 2003.

Dupuis M, KM Rosso, DM Smith, MS Gutowski, and JE Jaffe. 2003. "First-Principles Study of Metal Oxides: Electron Transport in Oxides." Presented by Michel Dupuis (Invited Speaker) at University of Hiroshima - Quantum Life Sciences, Hiroshima, Japan, on November 20, 2003.

Engelhard MH, DR Baer, D Kim, and DJ Gaspar. 2003. "Test Studies on Charging, Charge Compensation and XPS Binding Energy Referencing for Al-O_x on Al and SiO₂." Presented by Mark Engelhard at the American Vacuum Society's 50th International Symposium, Baltimore, Maryland, on November 2, 2003.

Gao F, EJ Bylaska, A El-Azab, and WJ Weber. 2003. "Comparative Study of Defect Properties in GaN: Ab Initio and Empirical-Potential Calculations." Presented by Fei Gao at the Materials Research Society Fall Meeting (Symposium on Radiation Effects and Ion Beam Processing of Materials), Boston, Massachusetts, on December 2, 2003.

Gao F, M Posselt, WJ Weber, and V Belko. 2003. "Atomic Computer Simulations of Defect Migration in SiC." Presented by Fei Gao at the International Conference on Silicon Carbide and Related Materials 2003, Lyon, France, on October 6, 2003.

Gaspar DJ, MH Engelhard, DE McCready, AA Rouse, and C Szeles. 2003. "Chemical Structure of the Pt/CdZnTe Interface." Presented by Daniel J. Gaspar at the American Vacuum Society's 50th International Symposium, Baltimore, Maryland, on November 2, 2003.

Grate JW. 2003. "Polymer Design and Analytical Chemistry for Sensor Arrays." Presented by Jay W. Grate (Invited Speaker) at the University of Nevada, Reno, Reno, Nevada, on November 22, 2003.

Henderson MA, J Szanyi, and JM White. 2003. "Photo-oxidation of Trimethyl Acetic Acid on the Surface of TiO₂(110)." Presented by M.A. Henderson at the 50th National Symposium of the American Vacuum Society, Baltimore, Maryland, on November 4, 2003.

Jiang W, WJ Weber, Y Zhang, LM Wang, and K Sun. 2003. "Irradiation-Induced Recovery of Disorder in Gallium Nitride and Silicon Carbide." Presented by Weilin Jiang at the Materials Research Society Fall Meeting (Symposium on Radiation Effects and Ion Beam Processing of Materials), Boston, Massachusetts, on December 2, 2003.

Jones DR, KA Perrine, ER Jurrus, BD Moon, and GM Petrie. 2003. "PiCEIS." Presented by Donald R. Jones (Invited Speaker) at a Technical Seminar Series - University of Utah Computing and Engineering Department, Salt Lake City, Utah, on November 13, 2003.

Jones DR. 2003. "Molecular Science Computing Facility: A Resource for Computational Research." Presented by Donald R. Jones (Invited Speaker) at a Distinguished Alumni Seminar Series - Brigham Young University, Provo, Utah, on November 14, 2003.

Kaspar TC, TC Droubay, AC Tuan, CM Wang, SA Chambers, and JW Rogers. 2003. "Materials Characterization and Magnetic Studies of Epitaxial Co_xTi_{1-x}O_{2-x} Deposited on Si(001) by Molecular Beam Epitaxy." Presented by Tiffany Kaspar at the American Vacuum Society's 50th International Symposium, Baltimore, Maryland, on November 4, 2003.

Lea AS, MH Engelhard, and DR Baer. 2003. "Comparison of X-ray and Electron Beam Induced Damage Rates." Presented by Scott Lea at the American Vacuum Society's 50th International Symposium, Baltimore, Maryland, on November 2, 2003.

Lyubinetsky IV, S Thevuthasan, AS Lea, DE McCready, and DR Baer. 2003. "Initial Stages of Cu₂O Nano-Clusters Formation on SrTiO₃(100)1." Presented by I. Lyubinetsky at the American Vacuum Society's 50th International Symposium, Baltimore, Maryland, on November 3, 2003.

Pecher KH, DR Baer, and MH Engelhard. 2003. "Iron-Oxide Nanoparticle Stability in an Ion Beam." Presented by D.R. Baer at the 50th American Vacuum Society's International Symposium, Baltimore, Maryland, on November 3, 2003.

Peden CHF, S Azad, MH Engelhard, MA Henderson, J Szanyi, and LQ Wang. 2003. "The Adsorption and Reaction of NO on Single Crystal Titanate (TiO₂ and SrTiO₃) Surfaces." Presented by Charles Peden at the 50th American Vacuum Society International Symposium, Baltimore, Maryland, on November 3, 2003.

Posselt M, F Gao, WJ Weber, and V Belko. 2003. "Influence of Polytypism on Properties of Intrinsic Defects in SiC." Presented by Matthias Posselt at the International Conference on Silicon Carbide and Related Materials 2003, Lyon, France, on October 6, 2003.

Qafoku N, CC Ainsworth, RK Kukkadapu, A Dohnalkova, and O Qafoku. 2003. "Fe-Solid Phase Transformations in the Sediments Under Hyperalkaline and Saline Conditions." Presented by Nik Qafoku at ASA-CSSA-SSSA 2003 Annual Meeting, Denver, Colorado, on November 2, 2003.

Saraf LV, V Shutthanandan, CM Wang, KT Koch, OA Marina, and S Thevuthasan. 2003. "Correlation of Oxygen Diffusivity with Grain-Boundary Dynamics and Its Impact on Ionic Migration in Doped Nano-crystalline CeO₂ Films." Presented by Laxmikant Saraf at the Materials Research Society Meeting, Boston, Massachusetts, on December 3, 2003.

Szanyi J, MA Henderson, and JM White. 2003. "The Origin of Photo-Induced Hydrophilicity on TiO₂ Surfaces: Photo-Generation of Surface Oxygen Vacancies or Photo-Oxidation of Adsorbed Organics." Presented by J. Szanyi at the American Vacuum Society Symposium, Baltimore, Maryland, on November 4, 2003.

Wang C, S Shutthanandan, Y Zhang, S Thevuthasan, and DR Baer. 2003. "Microstructure of Precipitated Au Nano Clusters in TiO₂." Presented by C. Wang (Invited Speaker) at the Materials Research Society 2003 Fall Meeting, Boston, Massachusetts, on December 1, 2003.

Windus TL. 2003. "CINF 92 Collaboratory for Multi-scale Chemical Science." Presented by Theresa Windus (Invited Speaker) at US-Russian Workshop on Software, Tempe, Arizona, on November 13, 2003.

Windus TL. 2003. "Molecular Science Software Group – at Super Computing 2003." Presented by Theresa Windus at Supercomputing 2003, Phoenix, Arizona, on November 17, 2003.

Zhang H, CM Wang, and L Wang. 2003. "Synthesis of Amorphous Helical SiO₂." Presented by CM Wang (Invited Speaker) at the Material Research Society 2003 Fall Meeting, Boston, Massachusetts, on December 1, 2003.